PANCREAS

CT perfusion as a potential biomarker for pancreatic ductal adenocarcinoma during routine staging and restaging

Ryan B. O'Malley[1] · Danielle Cox[1] · Erik V. Soloff[1] · Mladen Zečević[1] · Steven Green[2] · Andrew Coveler[2] · Janet M. Busey[1] · Carolyn L. Wang[1]

Abstract

Purpose To evaluate the significance of CT perfusion parameters predicting response to neoadjuvant therapy in patients with pancreatic ductal adenocarcinoma (PDAC).

Materials and methods Seventy patients with PDAC prospectively had CT perfusion acquisition incorporated into baseline multiphase staging CT. Twenty-eight who were naïve to therapy were retained for further investigation. Perfusion was performed 5–42.5 s after contrast, followed by parenchymal and portal venous phases. Blood flow (BF), blood volume (BV), and permeability surface area product (PS) were calculated using deconvolution algorithms. Patients were categorized as responders or non-responders per RECIST 1.1. Perfusion variables with AUC ≥ 0.70 in differentiating responders from non-responders were retained. Logistic regression was used to assess associations between baseline perfusion variables and response.

Results 18 of 28 patients showed favorable response to therapy. Baseline heterogeneity variables in tumor max ROI were higher in non-responders than responders [median BF coefficient of variation (CV) 0.91 vs. 0.51 respectively, odds ratio (OR) 6.8 per one standard deviation (1-SD) increase, $P = 0.047$; median PS CV 1.6 vs. 0.68, OR 3.9 per 1-SD increase, $P = 0.047$; and median BV CV 0.75 vs. 0.54, OR = 4.0 per 1-SD increase, $P = 0.047$]. Baseline BV mean in tumor center was lower in non-responders than responders (median BV mean: 0.74 vs. 2.9 ml/100 g respectively, OR 0.28 per 1-SD increase, $P = 0.047$).

Conclusion For patients with PDAC receiving neoadjuvant therapy, lower and more heterogeneous perfusion parameters correlated with an unfavorable response to therapy. Such quantitative information can be acquired utilizing a comprehensive protocol interleaving perfusion CT acquisition with standard of care multiphase CT scans using a single contrast injection, which could be used to identify surgical candidates and predict outcome.

✉ Ryan B. O'Malley
ryanomal@uw.edu

1 Department of Radiology, University of Washington School of Medicine, 1959 NE Pacific St, Box 357115, Seattle, WA 98195, USA

2 Seattle Cancer Care Alliance, 825 Eastlake Ave E, Seattle, WA 98109, USA
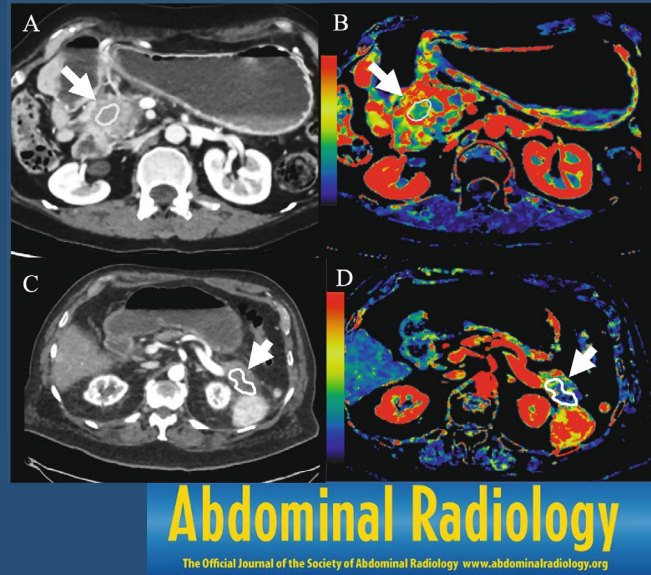
Graphical abstract

CT Perfusion as a Potential Biomarker for Pancreatic Ductal Adenocarcinoma During Routine Staging and Restaging

28 patients with PDAC naïve to prior treatment prospectively had a CT perfusion acquisition incorporated into baseline multiphase staging CT using the same IV contrast injection.

Lower and more heterogeneous perfusion parameters in the tumor were associated with unfavorable response to therapy.

Figure: Pancreatic head mass with higher perfusion and lower heterogeneity (A, B) showed stable disease at follow-up whereas mass in the tail with lower perfusion and higher heterogeneity (C, D) showed progressive disease.

O'Malley RB et al. 2022

Abdominal Radiology
The Official Journal of the Society of Abdominal Radiology www.abdominalradiology.org

Abbreviations

PDAC	Pancreatic ductal adenocarcinoma
ROI	Region of interest
AUC	Area under the receiver operating characteristic curve
IQR	Interquartile range
CV	Coefficient of variation
CT	Computed tomography
BR	Borderline resectable
LA	Locally advanced
BV	Blood volume
PS	Permeability surface area product
BF	Blood flow
TTP	Time to peak concentration
CA	Carbohydrate antigen
$CTDI_{vol}$	CT dose index
SSDE	Size specific dose index

Introduction

Prognosis for pancreatic ductal adenocarcinoma (PDAC) remains poor with 5-year survival rate of less than 10% and its incidence continues to increase such that it is now the third leading cause of cancer death in the USA [1–3]. Moreover, 5-year survival has remained unchanged even though more patients now present with resectable disease and are able to undergo ostensibly a curative resection [4–6]. For patients with locally advanced (LA) and borderline resectable (BR) PDAC, resection is usually deferred following neoadjuvant therapy ultimately still with the hope of achieving an R0 resection [6]. Imaging findings of resectability at baseline become increasingly unreliable after neoadjuvant therapy and have been shown not to be predictive of an R0 resection [7, 8]. As such, some institutions advocate for surgical exploration for all BR and LA patients that do not have evidence of progression during neoadjuvant therapy [7]. This highlights the need for noninvasive quantitative markers to more accurately predict response to neoadjuvant therapy, ideally using techniques that can be acquired in parallel with the standard of care multiphase CT.

Volume perfusion CT is a specific noninvasive CT technique that measures dynamic changes in tissue iodine concentration (IC) over time. Using postprocessing, tissue-specific parameters can be calculated, including blood flow (BF), blood volume (BV), time to peak concentration (TTP), vascular permeability surface area product (PS), and permeability (K_{trans}), which have many potential applications in oncologic imaging,

such as grading tumors at baseline, assessing response to neo-adjuvant therapy, and distinguishing viable from nonviable tumor prior to surgical resection [9, 10]. For PDAC, most tumors are hypovascular and hypoenhancing and quantifying the degree of perfusion may offer a better way to predict response. Hypoenhancement on CT is an independent negative predictor of survival and implies the presence of fibrosclerotic stroma, which is thought to result in a worse response to systemic therapy due to intratumoral hypoxia, hypoperfusion, and fibrosis [11]. Perfusion CT has already been used in patients with PDAC to differentiate between high- and low-grade tumors and also to assess response to neoadjuvant therapy, although always using dedicated perfusion CT acquisitions separate from the standard of care CT [12, 13]. Needing a second intravenous contrast injection separate from the standard of care CT is one factor that has limited more widespread adoption, along with other historical technical limitations such as high radiation dose, time added, and respiratory motion *n*.

We sought to evaluate the significance of perfusion parameters in PDAC for patients undergoing staging and restaging on a 256-slice 160 mm wide-detector scanner. It has been shown recently that it is feasible to acquire perfusion parameters concurrently with standard of care multiphase CT imaging for staging and restaging, without affecting image quality, at an acceptable radiation dose, and without adding cost or time to the scan [14, 15]. Using these methods, we sought to test the significance of a single comprehensive examination for PDAC by providing essential qualitative and quantitative data at each follow-up time point without using a separate scan or IV contrast injection. Secondarily, we compared carbohydrate antigen (CA) 19-9 to both RECIST and perfusion to explore the ability of CA 19-9 to predict outcomes and track progression of disease over time.

Demonstrating the significance of perfusion parameters for PDAC acquired concurrently during routine CT offers the potential for a new standard of care with a single examination providing all essential qualitative and quantitative information. Increased utilization could help establish cutoff values that might distinguish between responders and non-responders, determine timing of surgery, and help clarify residual viable and non-viable neoplasm, thus identifying patients that ordinarily would be precluded from curative intent resection. Establishing the significance of perfusion parameters using consistent techniques is the first step in laying the groundwork for future research, both in PDAC and other solid tumors.

Materials and methods

Patients

Institutional Review Board approval was obtained for this prospective HIPAA-compliant investigator-initiated study.

Between February 2018 and March 2021, 70 patients with pathologically proven PDAC undergoing a pancreas staging or restaging CT were prospectively identified and written informed consent was obtained. Exclusion criteria included patients unable to provide proper informed consent, women who were pregnant or intending to become pregnant during the study, patients with body mass index (BMI) greater than 40 kg/m^2, and patients with a history of severe allergic-like reaction to iodinated contrast media.

Image acquisition

All CT exams were performed on a 160 mm wide-detector 256-slice scanner (Revolution CT, GE Healthcare, Waukesha, WI). A weight-based dose of intravenous contrast (Omnipaque 350; GE Healthcare, Chalfont St. Giles, UK) was administered through a dual-head power injector (Stelland D; Medrad, Warrendale, PA) at a preferred injection rate of 5 ml/s. Patients with pre-existing implanted port catheters had contrast injected at a maximum rate of 4.2 ml/s. Beginning 5 s after intravenous contrast injection, a 37.5 s perfusion acquisition was performed from 5 to 42.5 s (15 passes at 2.5 s intervals with slow and shallow breathing) followed by fixed timing routine pancreatic parenchymal (45 s) and abdomen pelvis portal venous phase (70 s) acquisitions that were pushed to PACS and interpreted for routine clinical care (PACS; Centricity, GE Healthcare, Chicago, IL). Additional details of the CT protocol and scan parameters are outlined in Table 1 and Fig. 1. After the baseline CT, timing and frequency of follow-up CT was determined by the standard of care during treatment. Perfusion acquisitions were performed at each follow-up timepoint. The last follow-up CT for each patient was considered the final follow up (FFU).

Radiation dose calculations

CT dose index (CTDI$_{vol}$) and dose length product (DLP) were recorded for each CT exam. The estimated effective radiation dose was calculated using the conversion coefficient for the abdomen 0.015 [16]. Size-specific dose estimate (SSDE) was calculated using the sum of the anterior–posterior and lateral dimensions at the level of the pancreas [17].

Data analysis

Perfusion data for both baseline and subsequent follow-up perfusion acquisitions were analyzed using dedicated software (CT perfusion 4D; AW Server; GE Medical Systems) after applying a motion correction algorithm. Regions of interest (ROI) were drawn freehand by a single radiologist (XXX, fellowship trained in abdominal imaging with 12 years of experience in radiology) and placed in the

Table 1 CT exam and post-processing parameters

	Perfusion	Pancreatic	Portal venous
Scan mode	Axial	Axial	Axial
Noise index*	–	18	18
Detector coverage (mm)	160	140	140
Gantry rotation time (s)	0.5	0.5	0.5
Tube voltage (kVp)	100	120	120
Tube current mode	Manual	Smart	Smart
Tube current (mA)	140	80–500	80–450
Number of passes	15	1	1
Reconstruction slice thickness (mm)	2.5	2.5	2.5
Reconstruction slice interval (mm)	2.5	2.5	2.5
Reconstruction kernel	Standard	Standard	Standard
Noise reduction	ASIR-V 70%	ASIR-V 50%	ASIR-V 50%

ASIR adaptive statistical iterative reconstruction, *kVp* peak kilovoltage, *mA* milliampere

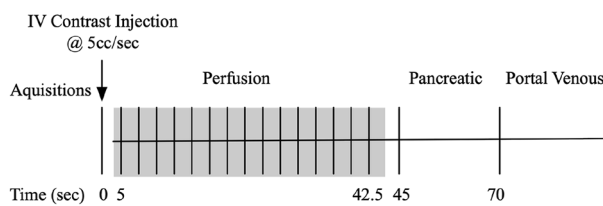*Noise index is based on a primary reconstruction of 2.5 mm

Fig. 1 Diagram of pancreas CT perfusion protocol. A weight-based contrast dose of 100–180 ml Omnipaque 350 was used with a preferred injection rate of 5 cm^3/s. Patients with preexisting port catheters received a maximum injection rate of 4.2 cm^3/s due to rate limitations. Fifteen perfusion acquisitions were obtained every 2.5 s beginning at 5 s (grey). Pancreatic parenchymal and portal venous acquisitions occurred at 45 and 70 s

suprarenal aorta, tumor, and pancreas. ROI for the tumor were drawn on the axial image(s) on the native exam where the mass was largest and/or had maximal contrast compared to adjacent pancreatic parenchyma. Three separate tumoral ROIs were drawn: (1) center of the tumor, (2) outer rim of the tumor, and (3) as large as possible to cover the entire tumor ("tumor max"), all of which were drawn while avoiding biliary or pancreatic stents, encased blood vessels, dilated pancreatic duct or side branches, and cystic components. In cases where there was uncertainty, the radiologist erred on the side of placing within clear tumor and avoiding normal parenchyma. Two ROIs were also placed in tumor-free uninvolved pancreas, one that was along the closest border with the tumor and one remote from the tumor, both avoiding blood vessels and atrophic parenchyma (Fig. 2). Identical ROIs were propagated to all perfusion phases to generate perfusion maps from which tumor BF, BV, and PS were calculated using deconvolution algorithms. We utilized the deconvolution model since it has been suggested that it can tolerate greater image noise and therefore measure lower levels of perfusion, as is the case with PDAC [18]. These variables were selected as they are the three parameters most frequently reported and considered to be most significant for PDAC [19]. 5 Parameters [min, max, mean, standard deviation (SD), and coefficient of variation (CV or heterogeneity)] were generated from the distributions of the 3 tissue-specific maps (i.e. BF, BV and PS) in the 6 ROIs—resulting in 90 perfusion variables to be used in further analysis. CV, a proxy measure of intratumor heterogeneity, was calculated by dividing the SD by the mean of a perfusion map. ROIs were numbered sequentially and images with the ROI sizes, shapes, and locations were saved in the perfusion software and exported as a comma separated values (CSV) file. Standard pancreatic arterial and venous phase images were reviewed in PACS as per routine clinical protocol. A separate radiologist (XXX fellowship trained in abdominal imaging with 19 years of experience in radiology) recorded the bidimensional tumor size and determined the response assessment using RECIST 1.1 criteria. Patients with stable disease or partial response were considered "responders" whereas patients with progressive disease were characterized as "non-responders." Perfusion variables at baseline were compared with treatment response (per RECIST 1.1). CA 19-9 levels were extracted from the electronic medical records at each timepoint. The baseline CA 19-9 levels were compared to both treatment response and pre-treatment levels of perfusion variables. Additionally, pre-post therapy changes in CA 19-9 levels were assessed separately in responders and non-responders to therapy.

Statistical analysis

Baseline non-imaging characteristics of patients with and without response to chemoradiation therapy were compared with the Fisher's exact test (categorical) or the Wilcoxon
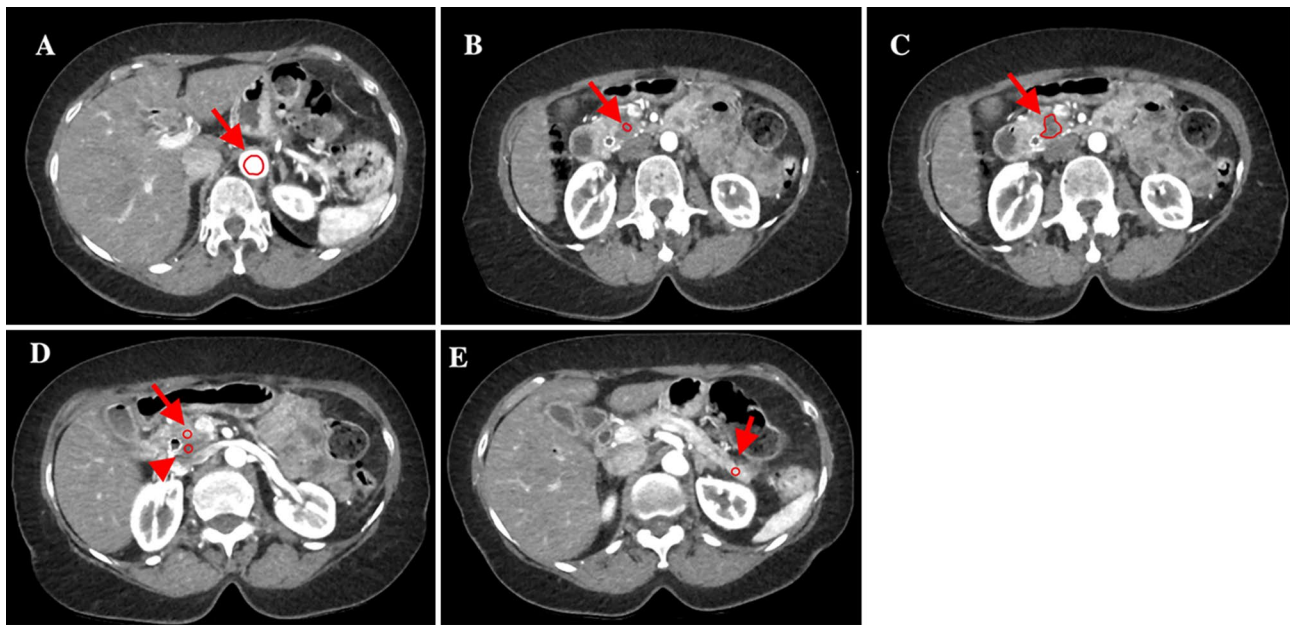
Fig. 2 Axial CT images demonstrating freehand ROIs drawn on **A** the suprarenal aorta, **B** the center of the pancreas tumor, **C** as large as possible to cover the entire pancreas tumor ("tumor max"), **D** the outer rim of the pancreas tumor (arrowhead) and tumor free unin-volved pancreas along the closest border with the tumor (arrow) and **E** uninvolved pancreas remote from the tumor. Identical ROIs were propagated to all perfusion phases to generate perfusion maps from which perfusion variables were calculated

rank-sum test (continuous variables). The Wilcoxon matched-pairs signed rank test was used to compare CA 19-9 values before and after therapy.

The sample size of 28 patients was not sufficient to bear the inferential analysis on 90 perfusion variables. Rather, a subset of perfusion variables was selected based on their univariable discriminative capacity. First, all of the 90 perfusion variables were ranked based on their ability to differentiate patients with and without response to therapy using the area under the receiver operating characteristics curve (AUC). Second, since generally discriminative performance of AUC ≥ 0.70 are considered acceptable, we retained only variables meeting this criterion [20]. Associations of the select baseline perfusion features with response to treatment were then assessed with univariable logistic regression models. All right-skewed perfusion variables were log-transformed prior to inclusion in their respective model. Following the log-transformation (when needed), the studied perfusion variables were z-transformed (i.e., zero-centered and divided by the SD). The z-transformation ensured that the computed odds ratios (ORs), summarizing the magnitudes of associations of individual perfusion variables with the disease status, were on the same scale (i.e., more comparable). Relationships between perfusion variables and non-imaging covariates (CA 19-9 and Age) were evaluated with Spearman correlation analysis. P values of all tests involving perfusion variables were adjusted for multiple comparisons with

Benjamini–Hochberg procedure, a more powerful alternative to Bonferroni correction [21]. Throughout, P values < 0.05 were indicative of significant effects.

Results

Patient cohort

For this analysis, 28 of the 70 patients who had perfusion CT were included in this cohort (median age 67 years; 15 men) as they were naïve to previous treatment (Fig. 3). Characteristics of these 28 patients are summarized in Table 2. Median FFU time was 125 days (IQR 78 to 211 days). Of the 28 patients, 14 (50%) had 1 follow-up CT after baseline, 6 (21%) had 2, 7 (25%) had 3, and 1 patient (4%) had 4 follow-up CT scans. Eighteen patients (64%) were considered responders (3 partial responses and 15 stable diseases, per RECIST 1.1) and 10 (36%) were considered non-responders (progressive diseases, per RECIST 1.1). Responders were older than non-responders (median age at baseline 71 vs. 58 years respectively, $P = 0.011$). The mean contrast dose was 138 mL (range 80 to 180 ml), mean iodine dose was 698.8 mg/kg (range 505.1 to 989.1 mg/kg) and the mean injection rate was 4.5 ml/s (range 3.5 to 6.0 ml/s). Estimated radiation doses for the perfusion, pancreatic, and portal venous phases are shown in Table 3.

Fig. 3 Flow diagram of recruitment. *FU1–FU4* 1st–4th follow-up timepoint
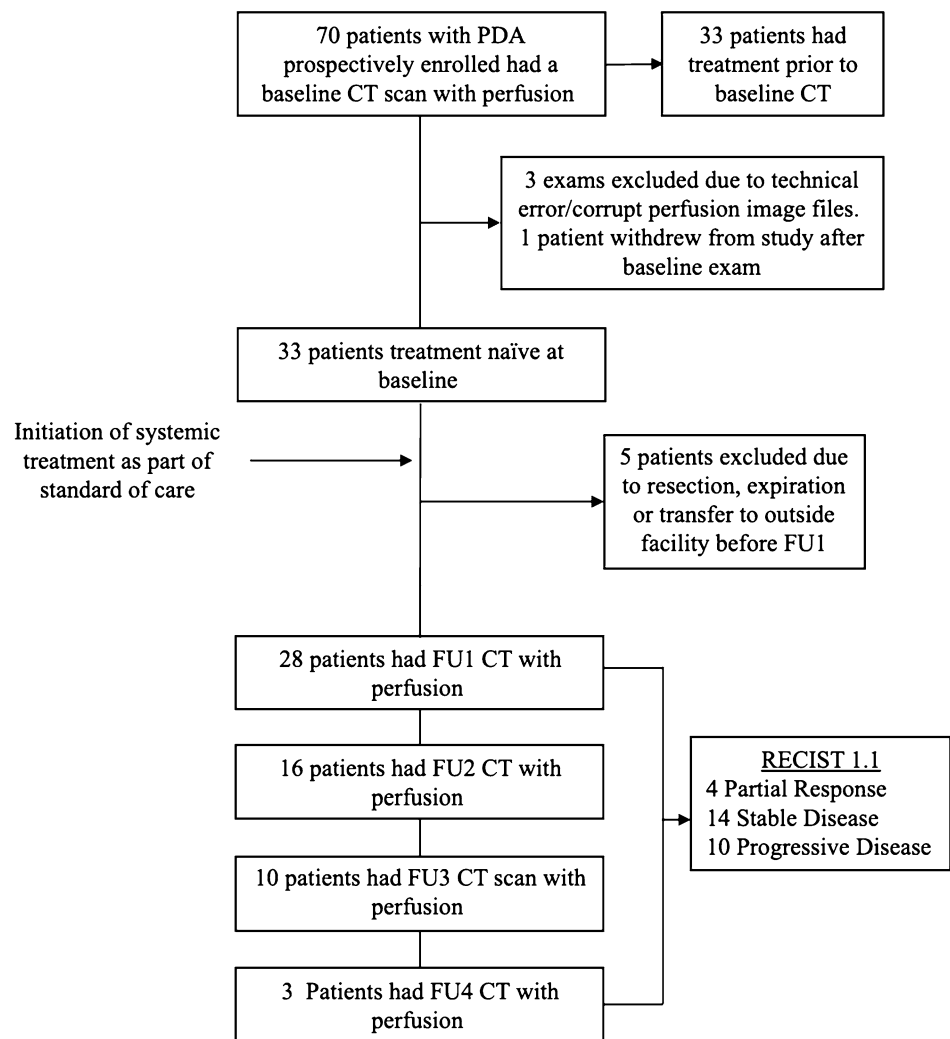
Perfusion variable selection

Of the 90 baseline perfusion variables tested, 9 met our retention criterion of AUC ≥ 0.70: three heterogeneity variables measured in tumor max ROI (BF CV, PS CV, and BV CV); four variables in tumor center (PS_{mean}, BV_{mean}, PS_{max}, and BF_{min}); one variable in tumor rim (BV_{mean}); and one variable in normal pancreas (PS CV). AUC values used for ranking of each perfusion variable are outlined in Table 4.

Associations of perfusion variables with disease status

Medians of all perfusion heterogeneity variables were observed to be larger in non-responders than responders to therapy, while this relationship reversed in min-, max-, and mean-based perfusion variables (Fig. 4; Table 4). Specifically, baseline BF, PS, and BV heterogeneities in tumor max ROI were higher in non-responders than responders to therapy (median BF CV 0.91 vs. 0.51 respectively, OR 6.8 per 1-SD increase, adjusted $P = 0.047$; median PS CV 1.6 vs. 0.68 respectively, OR 3.9 per 1-SD increase, adjusted $P = 0.047$; and median BV CV 0.75 vs. 0.54 respectively, OR 4.0 per 1-SD increase, adjusted $P = 0.047$). Likewise, PS CV in normal pancreas was higher in non-responders than responders to therapy, but this difference was not statistically significant (Table 4). On the other hand, baseline BV mean in tumor center was lower in non-responders than responders to therapy (median BV mean 0.74 vs. 2.9 ml/100 g respectively, OR 0.28 per 1-SD increase, adjusted $P = 0.047$). Similarly, PS_{max}, PS_{mean} and BF_{min}—all in tumor center, and BV mean in tumor rim were lower in non-responders than responders, but these effects were not statistically significant (Table 4).

As indicated earlier, patient age was significantly associated with the disease status. Nevertheless, the sample size was not sufficient to support multivariable regression analysis intended at studying effects of perfusion variables while statistically controlling for the age covariate. Instead, we used Spearman correlation analysis to explore whether

Table 2 Characteristics of PDA patients with and without response to therapy

Baseline variable	Overall† (n=28)	Responder to therapy*		P‡
		Yes† (n=18)	No† (n=10)	
Male sex	15 (54%)	9 (50%)	6 (60%)	0.71
Age (years)	67 (58–72)	71 (64–74)	58 (56–66)	**0.011**
BMI (kg/m²)	25 (22–27)	24 (21–27)	28 (25–29)	0.084
CA 19-9 (U/ml)	138 (19–855)	155 (25–689)	110 (12–5097)	0.72

FFU variable*	Overall† (n=28)	Responder to therapy*		P‡
		Yes† (n=18)	No† (n=10)	
Time from baseline (days)	125 (78–211)	117 (65–189)	150 (92–252)	0.16
Last follow-up time point				0.64
1	14 (50%)	10 (56%)	4 (40%)	
2	6 (21%)	4 (22%)	2 (20%)	
3	7 (25%)	4 (22%)	3 (30%)	
4	1 (4%)	0 (0%)	1 (10%)	
Disease status RECIST 1.1				-
Partial response	3 (11%)	–	–	
Stable disease	15 (53%)	–	–	
Progressive disease	10 (36%)	–	–	

Bold P-values indicate statistical significance

*Response to therapy was recorded at the most recent imaging time point within 9 months from baseline (FFU)

†Data are n (%) or median (interquartile range)

‡Fisher's exact test (categorical) or Wilcoxon rank-sum test (continuous variables) comparing patients with and without response to therapy

Table 3 Radiation doses

	Perfusion	Pancreatic	Portal venous
DLP (mGy cm)	743 ± 115 (529–1006)	431 ± 222 (85–1724)	918 ± 369 (354–1865)
CTDI$_{vol}$ (mGy)	46 ± 7 (33–62)	16 ± 7 (5–37)	14 ± 5 (5–30)
SSDE (mGy)	63 ± 12 (38–98)	21 ± 8 (10–40)	20 ± 6 (12–74)
Effective dose (mSv)	11 ± 2 (8–15)	6 ± 3 (1–26)	14 ± 5 (5–28)

Data are means ± standard deviations with range in parentheses. Effective dose was calculated using the abdominal conversion coefficient of 0.015

DLP dose length product, *CTDI$_{vol}$* CT dose index, *SSDE* size specific dose estimate

the four significant perfusion variables may be independent of age. Correlation of baseline age with BV CV in tumor max ROI was small, negative and non-significant ($r = -0.33$, adjusted $P = 0.36$). Correlations of age with BF CV ($r = -0.22$) and PS CV ($r = -0.20$) in tumor max ROI, and BV mean in tumor center ($r = -0.09$) were negligible (adjusted $P = 0.40$ to 0.65) (Supplemental Table 1).

CA 19-9

Correlations of CA 19-9 with the perfusion variables measured in tumor center ROI (i.e., PS$_{max}$, PS$_{mean}$, BF$_{min}$ and BV$_{mean}$) were negative, low in magnitude, and statistically non-significant ($r = -0.49$ to -0.31, adjusted $P = 0.078$ to

0.26). Correlations of the remaining five perfusion variables (measured in tumor max, tumor rim and normal pancreas) with CA 19-9 were negligible (adjusted $P = 0.55$ to 0.99) (Supplemental Table 1). Further, baseline CA 19-9 levels did not differ between responders and non-responders (median 155 vs. 110 U/ml respectively, $P = 0.72$) (Table 2).

CA 19-9 levels declined in responders after therapy (from a median of 155 [IQR 28–674] to 51 [IQR 9–163] U/ml; $P = 0.010$) but the change in CA 19-9 levels of non-responders was not significant (from a median of 110 [IQR 20–4020] to 663 [IQR 60–5658] U/ml; $P = 0.95$). However, 1 of 18 responders and 2 of 10 non-responders were missing CA 19-9 measurements at the FFU (Fig. 5).

Table 4 Baseline perfusion variables in Responders and Non-responders

ROI/perfusion variable		Response to therapy*		OR†	Adjusted P-value‡	AUC§
		Yes ($n = 18$)	No ($n = 10$)			
Tumor max						
Blood flow	CV	0.51 (0.40–0.57)	0.91 (0.56–1.0)	6.8 [1.7–27]	**0.047**	0.87
Permeability	CV	0.68 (0.57–1.0)	1.6 (1.0–2.5)	3.9 [1.3–12]	**0.047**	0.85
Blood volume	CV	0.54 (0.47–0.59)	0.75 (0.58–0.98)	4.0 [1.2–13]	**0.047**	0.76
Tumor center¶						
Blood flow	Min	13 (5.0–17)	2.0 (1.0–11)	0.45 [0.19–1.1]	0.093	0.70
Permeability	Max	17 (14–25)	8.1 (3.8–23)	0.53 [0.20–1.4]	0.21	0.71
	Mean	6.8 (5.2–14)	1.5 (1.0–11)	0.32 [0.10–1.0]	0.093	0.75
Blood volume	Mean	2.9 (2.3–3.5)	0.74 (0.57–3.2)	0.28 [0.10–0.80]	**0.047**	0.74
Tumor rim						
Blood volume	Mean	3.4 (2.0–4.7)	1.9 (1.2–4.0)	0.44 [0.17–1.1]	0.093	0.71
Normal pancreas#						
Permeability	CV	0.38 (0.26–0.73)	0.78 (0.54–1.2)	2.3 [0.92–5.9]	0.093	0.73

Bold P-values indicate statistical significance

OR odds ratio for progressive disease (nonresponse) per 1-SD increase in perfusion variable, *SD* standard deviation, *CV* coefficient of variation (heterogeneity), *ROI* region of interest, *AUC* area under the receiver operating characteristic curve. Response to therapy was recorded at the most recent imaging time point within 9 months from baseline. BF units = ml/100 g/min, BV units = ml/100 g, PS units = ml/100 g/min

*Data are median (interquartile range)

†Data in brackets are 95% confidence intervals

‡Wald-test P-value from logistic regression with Benjamini–Hochberg adjustment for multiple comparisons

§AUC values used for ranking of the perfusion variables; of the initial 90 perfusion variables, only those with AUC ≥ 0.70 are shown

¶1 of 10 non-responders was missing all of the perfusion measurements in tumor center ROI

#1 of 18 responders had a missing measurement for the perfusion variable

Discussion

Using a single comprehensive multiphase pancreas perfusion CT, our results show that higher perfusion parameters correlate with better outcomes for patients with PDAC. Specifically, an increase in mean BV in the tumor center ROI was significantly associated with decreasing likelihood of progressive disease. Additionally, increasing CV or heterogeneity of all three perfusion parameters (BF, BV, PS) were significantly associated with worse outcomes. Similar to Hamdy et al., we found no significant correlation with perfusion parameters and CA 19-9. By combining perfusion CT with standard of care CT, our approach utilizes a single IV contrast injection, adds no time or cost to the patient, while simultaneously acquiring quantitative data and standard of care staging and restaging information. PDAC perfusion CT technique is widely varied in the literature, but all current publications have acquired perfusion CT separately from the standard of care CT, thus requiring a separate scan and IV contrast injection. Such technical inconsistency and logistical barriers have prevented more widespread utilization, both for research and routine practice. However, recent work has shown that it is feasible to perform a perfusion CT acquisition concurrently with the standard of care CT scans using a single contrast injection and without detrimentally affecting the standard pancreatic and venous phases [14, 15]. This approach offers potential for more widespread utilization by acquiring perfusion information concurrently with the standard of care examination.

Our findings further substantiate the important role of CT perfusion in diagnosis, staging, and treatment assessment for patients with PDAC. Perfusion CT has already been used to show a significant difference in BV and BF between high- and low-grade tumors at baseline [12, 22]. Lower perfusion parameters in the tumor have also been used to identify PDAC from uninvolved pancreas, which is thought to reflect the fibrosis and extracellular matrix deposition associated with PDAC [13, 23]. In patients receiving neoadjuvant therapy, our results are similar to Hamdy et al. showing that patients with PDAC and higher perfusion parameters at baseline were more likely to respond to neoadjuvant therapy. This suggests that higher tumor perfusion is associated with a less rigid extracellular matrix and may result in improved delivery of systemic therapy.
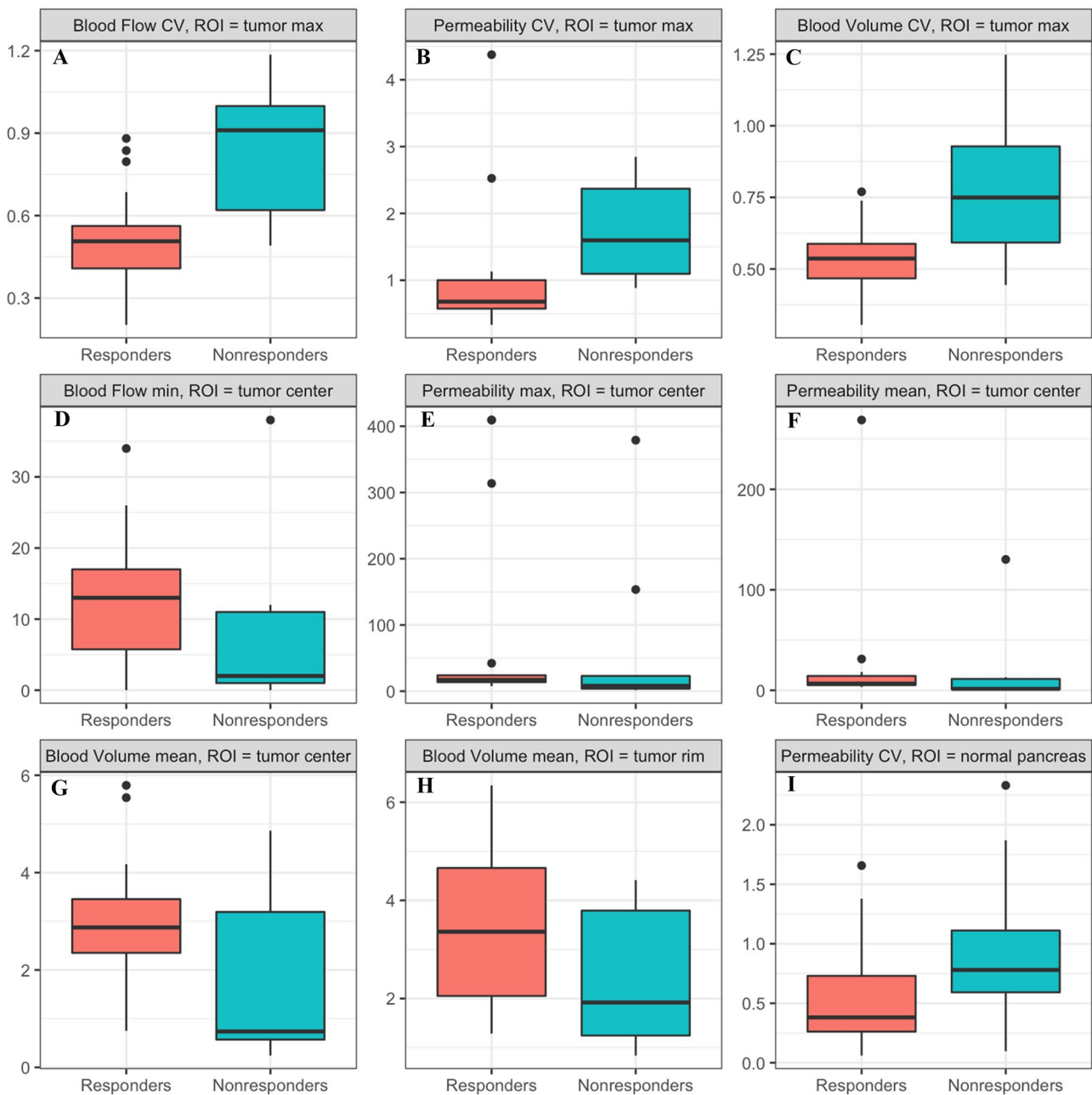
Fig. 4 Box plots summarizing pretherapy distributions of select perfusion features in PDAC patients with and without response to therapy. The horizontal lines across the boxes represent medians. Lower and upper edges of the boxes represent 25th and 75th percentiles. The upper and lower whiskers represent data outside the middle 50%. The dots represent outlying data points. *CV* coefficient of variation (heterogeneity), BF units = ml/100 g/min, BV units = ml/100 g, PS units = ml/100 g/min. Overall, pretherapy perfusion heterogeneity levels were higher in non-responders than responders to therapy (**A–C, I**), while this relationship reversed in min-, max-, and mean-based perfusion variables (**D–H**)

Moreover, we found that increasing perfusion heterogeneity also conferred a lower likelihood of responding to therapy. Intratumoral heterogeneity is an avid area of ongoing research as it is increasingly recognized as a poor prognostic factor, mechanism for resistance to anticancer therapy, and major driver of tumor progression [24]. This can manifest

as spatial heterogeneity, where there is an uneven distribution of features within the primary tumor, or temporal heterogeneity, where the makeup of a single lesion changes over time as it is exposed to various clinical interventions [25]. However, quantifying spatial or temporal heterogeneity typically requires biopsy or other invasive methods that are
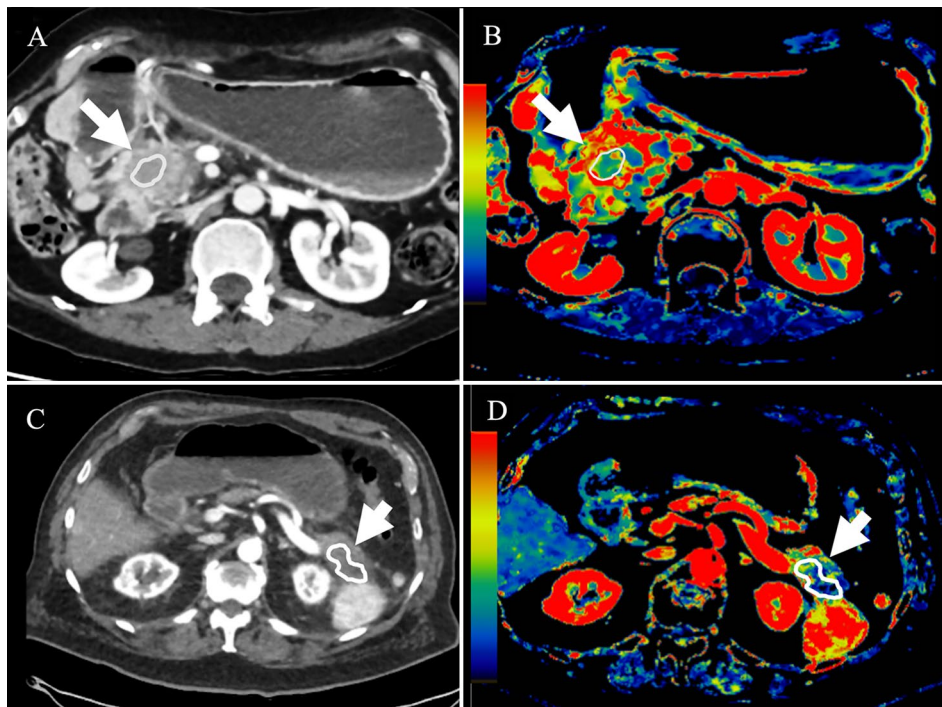
Fig. 5 A–D Images in two patients with pancreatic ductal adenocarcinoma (PDAC) showing high and low blood flow mean (BF_{mean}) and inversely low and high respective blood flow heterogeneity (BF CV). Baseline axial CT image (**A**) and perfusion BF color map (**B**) from a 50-year-old female with PDAC in the pancreatic head who showed stable disease at final follow-up. Freehand ROI (arrow) encompasses primary tumor max with BF mean = 59 ml/100 ml/min (high perfu-sion) and BF CV = 0.54 (low heterogeneity). Baseline axial CT image (**C**) and perfusion BF color map (**D**) from a 72-year-old male with PDAC in the tail who showed progressive disease at final follow-up. Freehand ROI (arrow) encompasses primary tumor max with BF mean = 7.4 ml/100 ml/min (low perfusion) and BF CV = 1.1 (high heterogeneity)

not practical for routine patient care. Imaging is uniquely positioned to offer comprehensive noninvasive assessment of tumor heterogeneity that can be used for effective treatment decision-making. Recently, a CT-based radiomics signature was developed that allowed for stratification of patients most likely to benefit from immune checkpoint inhibitors [26]. Within their model, tumor homogeneity was associated with higher likelihood of response. Using perfusion CT at baseline and each timepoint during therapy can add such predictive information not currently available with routine CT.

Although the potential for using tumor heterogeneity is established in some tumors, existing evidence in PDAC is still unclear. By using postprocessing software to quantitatively assess tumor heterogeneity at baseline and during treatment, texture analysis (TA) is increasingly utilized in oncologic patients and may provide additional biomarkers that prove to be useful for patients with PDAC [27]. However, existing evidence is limited and potentially conflicting. Sandrasegaran et al. correlated with TA to correlate with overall and progression-free survival and found that higher mean value of positive pixels (MPP) was significantly associated with worse survival [28]. By contrast, Borhani et al. correlated TA parameters in patients with potentially

resectable PDAC with histologic grading of tumor response and found that higher MPP at baseline was associated with increased likelihood of favorable treatment response [29]. Such apparently conflicting findings are examples of the wide variability that exists in published TA data and highlights the need for more studies and more consistency when evaluating tumor heterogeneity for PDAC.

Dual-energy CT (DECT) is another technique that has shown promise as a potential biomarker for evaluating PDAC. DECT is already established as a useful method for increased detection and conspicuity of PDAC using low keV monochromatic images [30]. There is also some evidence that quantitative markers on DECT correlate with perfusion parameters. Bao et al. found moderate positive correlation of BF and BV with IC for both PDAC and uninvolved pancreatic parenchyma [31]. Stiller et al. also found high correlation between IC and perfusion parameters, although their technique and calculations relied upon a patient-specific optimum time of acquisition (t_{opt}), which may not be feasible for all institutions [32]. Nonetheless, using DECT IC as a surrogate or replacement for perfusion parameters is a promising area that could make routine quantitative assessment even more widespread.

This study has several important limitations. First, our sample size was small and limited to 28 patients with PDAC who had not received prior treatment. A larger sample size would be required to validate our findings and correlate with outcomes. These patients did not receive the same treatment regimens and had different follow-up schedules, which reflected the clinical decision-making. Second, this protocol was performed on a single vendor wide-detector scanner as a reflection of our standard clinical workflow. However, it is not known whether these results apply to other vendors, scanner models, or scan parameters. Our specific protocol was only feasible for patients with BMI less than 40 kg/m^2, which limits the relevance for larger patients with higher BMI. Third, we used RECIST 1.1 to assess response, which is known to have limitations in patients with PDAC. If possible, correlating with histologic response on a resection specimen would be more appropriate, but is often not possible as a minority of patients undergo resection in most practices. Fourth, perfusion ROIs were placed by a single radiologist, therefore we cannot assess the reproducibility among other radiologists. Multiple readers could help to ensure that this process and the parameters are reproducible. Fifth, CT perfusion still suffers from a lack of reference values and technical standards. It is not possible to directly compare perfusion values across different scanners, mathematical models, and software used. Calculated perfusion parameters depend heavily on the kinetic model, which all use different assumptions and are not directly interchangeable [33]. Lastly, generating and analyzing perfusion parameters requires software separate from the clinical PACS, which adds time for the radiologist.

Conclusions

In conclusion, for patients with PDAC undergoing neoadjuvant therapy, lower and more heterogeneous perfusion parameters correlated with an unfavorable response to therapy. Such quantitative information can be acquired utilizing a protocol interleaving a perfusion CT acquisition with standard of care multiphase CT scans using a single contrast injection. Using updated CT technology, respiratory motion, image noise, and added radiation dose are no longer significant concerns, such that perfusion CT can be considered as an add-on for patients with PDAC. By acquiring predictive quantitative information as part of a single routine scan, we hope that perfusion CT can be increasingly utilized such that future research efforts can evaluate perfusion data in larger cohorts and ultimately help guide treatment decision-making.

Declarations

References

1. Nelson DW, Chang S-C, Grunkemeier G, et al. Resectable Distal Pancreas Cancer: Time to Reconsider the Role of Upfront Surgery. *Ann Surg Oncol.* 2018;25(13):4012–4019.
2. Zhong J, Switchenko J, Behera M, et al. Chemotherapy with or Without Definitive Radiation Therapy in Inoperable Pancreatic Cancer. *Ann Surg Oncol.* 2018;25(4):1026–1033.
3. Anon. Cancer of the Pancreas - Cancer Stat Facts. *SEER.* Available at: http://seer.cancer.gov/statfacts/html/pancreas.html. Accessed July 18, 2019.
4. Luberice K, Downs D, Sadowitz B, et al. Has survival improved following resection for pancreatic adenocarcinoma? *The American Journal of Surgery.* 2017;214(2):341–346.
5. Cassinotto C, Mouries A, Lafourcade J-P, et al. Locally advanced pancreatic adenocarcinoma: reassessment of response with CT after neoadjuvant chemotherapy and radiation therapy. *Radiology.* 2014;273(1):108–116.
6. Ferrone CR, Marchegiani G, Hong TS, et al. Radiological and surgical implications of neoadjuvant treatment with FOLFIRINOX for locally advanced and borderline resectable pancreatic cancer. *Ann Surg.* 2015;261(1):12–17.
7. Michelakos T, Pergolini I, Castillo CF, et al. Predictors of Resectability and Survival in Patients With Borderline and Locally Advanced Pancreatic Cancer who Underwent Neoadjuvant Treatment With FOLFIRINOX. *Annals of Surgery.* 2019;269(4):733–740.
8. Katz MHG, Fleming JB, Bhosale P, et al. Response of borderline resectable pancreatic cancer to neoadjuvant therapy is not reflected by radiographic indicators. *Cancer.* 2012;118(23):5749–5756.
9. Klotz E, Haberland U, Glatting G, et al. Technical prerequisites and imaging protocols for CT perfusion imaging in oncology. *Eur J Radiol.* 2015. Available at: http://linkinghub.elsevier.com/retrieve/pii/S0720048X15300176.
10. Prezzi D, Khan A, Goh V. Perfusion CT imaging of treatment response in oncology. *Eur J Radiol.* 2015;84(12):2380–2385.
11. Fukukura Y, Takumi K, Higashi M, et al. Contrast-enhanced CT and diffusion-weighted MR imaging: Performance as a prognostic factor in patients with pancreatic ductal adenocarcinoma. *Eur J Radiol.* 2014;83(4):612–619.
12. D'Onofrio M, Gallotti A, Mantovani W, et al. Perfusion CT can predict tumoral grading of pancreatic adenocarcinoma. *Eur J Radiol.* 2013;82(2):227–233.
13. Hamdy A, Ichikawa Y, Toyomasu Y, et al. Perfusion CT to Assess Response to Neoadjuvant Chemotherapy and Radiation Therapy in Pancreatic Ductal Adenocarcinoma: Initial Experience. *Radiology.* 2019:182561.

14. Konno Y, Hiraka T, Kanoto M, et al. Pancreatic perfusion imaging method that reduces radiation dose and maintains image quality by combining volumetric perfusion CT with multiphasic contrast enhanced-CT. *Pancreatology*. 2020. Available at: http://www.sciencedirect.com/science/article/pii/S1424390320306591. Accessed September 8, 2020.

15. O'Malley RB, Soloff EV, Coveler AL, et al. Feasibility of wide detector CT perfusion imaging performed during routine staging and restaging of pancreatic ductal adenocarcinoma. *Abdom Radiol*. 2021;46(5):1992–2002.

16. AAPM Task Group 23. AAPM Report No. 96 The Measurement, Reporting, and Management of Radiation Dose in CT. *AAPM Report No. 96 The Measurement, Reporting, and Management of Radiation Dose in CT*. 2008. Available at: https://www.aapm.org/pubs/reports/RPT_96.pdf. Accessed January 2, 2020.

17. AAPM Task Group 204. AAPM Report No. 204 Size-Specific Dose Estimates (SSDE) in Pediatric and Adult Body CT Examinations. *Size-Specific Dose Estimates (SSDE) in Pediatric and Adult Body CT Examinations*. 2011. Available at: https://www.aapm.org/pubs/reports/rpt_204.pdf. Accessed January 2, 2020.

18. Miles KA. Perfusion CT for the assessment of tumour vascularity: which protocol? *BJR*. 2003;76(suppl_1):S36–S42.

19. Aslan S, Nural MS, Camlidag I, et al. Efficacy of perfusion CT in differentiating of pancreatic ductal adenocarcinoma from mass-forming chronic pancreatitis and characterization of isoattenuating pancreatic lesions. *Abdom Radiol*. 2019;44(2):593–603.

20. David W. Hosmer, Stanley Lemeshow. *Applied Logistic Regression*. 2nd ed. New York, NY: John Wiley and Sons; 2000.

21. Hochberg Y, Benjamini Y. More powerful procedures for multiple significance testing. *Stat Med*. 1990;9(7):811–818.

22. Kovač JD, DJurić-Stefanović A, Dugalić V, et al. CT perfusion and diffusion-weighted MR imaging of pancreatic adenocarcinoma: can we predict tumor grade using functional parameters? *Acta Radiologica*. 2018:028418511881220–9.

23. Perik TH, van Genugten EAJ, Aarntzen EHJG, et al. Quantitative CT perfusion imaging in patients with pancreatic cancer: a systematic review. *Abdom Radiol*. 2021. Available at: https://doi.org/10.1007/s00261-021-03190-w. Accessed July 9, 2021.

24. Caswell DR, Swanton C. The role of tumour heterogeneity and clonal cooperativity in metastasis, immune evasion and clinical outcome. *BMC Medicine*. 2017;15(1):133.

25. Dagogo-Jack I, Shaw AT. Tumour heterogeneity and resistance to cancer therapies. *Nat Rev Clin Oncol*. 2018;15(2):81–94.

26. Ligero M, Garcia-Ruiz A, Viaplana C, et al. A CT-based Radiomics Signature is Associated with Response to Immune Checkpoint Inhibitors in Advanced Solid Tumors. *Radiology*. 2021;299(1):109–119.

27. Lubner MG, Smith AD, Sandrasegaran K, et al. CT Texture Analysis: Definitions, Applications, Biologic Correlates, and Challenges. *RadioGraphics*. 2017;37(5):1483–1503.

28. Sandrasegaran K, Lin Y, Asare-Sawiri M, et al. CT texture analysis of pancreatic cancer. *Eur Radiol*. 2019;29(3):1067–1073.

29. Borhani AA, Dewan R, Furlan A, et al. Assessment of Response to Neoadjuvant Therapy Using CT Texture Analysis in Patients With Resectable and Borderline Resectable Pancreatic Ductal Adenocarcinoma. *American Journal of Roentgenology*. 2020;214(2):362–369.

30. George E, Wortman JR, Fulwadhva UP, et al. Dual energy CT applications in pancreatic pathologies. *Br J Radiol*. 2017;90(1080):20170411.

31. Bao J, Liu A, Zhao C, et al. Correlation Between Dual-Energy Computed Tomography Single Scan and Computed Tomography Perfusion for Pancreatic Cancer Patients: Initial Experience. *Journal of Computer Assisted Tomography*. 2019:1.

32. Stiller W, Skornitzke S, Fritz F, et al. Correlation of Quantitative Dual-Energy Computed Tomography Iodine Maps and Abdominal Computed Tomography Perfusion Measurements: Are Single-Acquisition Dual-Energy Computed Tomography Iodine Maps More Than a Reduced-Dose Surrogate of Conventional Computed Tomography Perfusion? *Investigative Radiology*. 2015;50(10):703–708.

33. Schneeweiß S, Horger M, Grözinger A, et al. CT-perfusion measurements in pancreatic carcinoma with different kinetic models: Is there a chance for tumour grading based on functional parameters? *Cancer Imaging*. 2016;16(1):43.